Progress In Electromagnetics Research C, Vol. 66, 129–137, 2016

Gain Enhancement in Planar Monopole Antennas

Lin-Chuan Tsai*

Abstract—This paper proposes a planar monopole antenna design for achieving gain enhancement. The desired radiation pattern is achieved straightforwardly by employing a detached glass slab and placing a reflected metal slab after the glass slab onto the antenna structure. Geometrical parameters were examined to optimize the performance of the proposed antenna. Such a configuration causes constructive interference between the incident and reflected fields. The radiation patterns can be adjusted using the thickness of the glass slab and dielectric constants. The radiated fields are redistributed because of the inclusion of the glass slab, which has a permittivity of $\varepsilon_r = 7.75$ and a thickness of $h = 1\,\text{mm}$. Consequently, the planar monopole gain achieved using the glass slab and reflected metal slab increases to approximately 5 dBi, while the antenna resonant frequency remains almost unchanged at nearly 14% of impedance bandwidth. The results obtained for the directional pattern, return loss, gain, and radiation efficiency of the proposed antenna were analyzed. The volume of the antenna radiation area and ground plane is $3 \times 32 \times 52\,\text{mm}^3$. Detailed simulations and experiments were conducted to optimize the gain enhancement operations, and the measured results agreed with the simulated ones.

1. INTRODUCTION

Printed circuit antennas have been investigated extensively in recent years. To overcome the low-gain characteristics of circuit antennas, several gain enhancement methods have been proposed [1–11]. The design proposed by [1] forces constructive interference between the incident and reflected fields inside the substrate. Partially reflecting surface (PRS) antennas, which have attracted considerable interest in recent years, exhibit the advantage of high directivity and typically consist of a PRS material placed at approximately half a wavelength above a ground plane containing a source antenna. Numerous PRS antennas have been examined for enhancing gain [6–11]. In [6], thin, single-dielectric-slab PRSs with printed patterns on both sides were proposed for minimizing the PRS thickness and for simplifying fabrication, and PRSs exhibiting positive reflection phase gradients were investigated to design wideband, low-profile, electromagnetic band gap (EBG) resonator antennas. In this design, operating frequencies are electronically tuned by incorporating an array of phase-agile reflection cells on a thin substrate on the ground plane of a resonator antenna. High-gain PRS antennas exhibiting a reconfigurable operating frequency were presented in [7]. In [8], high-gain planar antennas were investigated by placing an optimized PRS in front of a waveguide aperture on a ground plane. Several other PRS antennas have been also proposed to enhance gain [9–11]. The PRS antennas in the above references exhibit high gain. However, the drawbacks of the PRS configuration are that the antennas require additional space because most PRS materials are placed at approximately half a wavelength above a ground plane, and that the antennas have high manufacturing costs and complicated structures.

This study developed and implemented a new configuration for designing an antenna to achieve gain enhancement. To obtain favorable impedance conditions and gain enhancement, the required

Received 3 May 2016, Accepted 22 July 2016, Scheduled 29 July 2016
* Corresponding author: Lin-Chuan Tsai (ginggle@mail.lhu.edu.tw).
The authors is with the Department of Electronic Engineering, Lunghwa University of Science and Technology, 300 Wanshou Rd., Sec. 1, Guishan Shiang, Taoyuan 33306, Taiwan, R.O.C.

geometrical configuration for the monopole antenna was derived by optimizing the thickness of the glass slab and dielectric constant of the glass slab as parameters. The proposed design procedures developed for the specified frequencies were validated by performing simulations and measurements. The performance of the proposed antenna was compared with that of the conventional monopole antenna (CMA) and for the different dielectric constants of the glass slab. The remainder of this paper is organized as follows: Section 2 describes the gain enhancement of the monopole antenna, and Section 3 discusses the experimental and simulated results obtained for the proposed antenna. Section 4 concludes the paper.

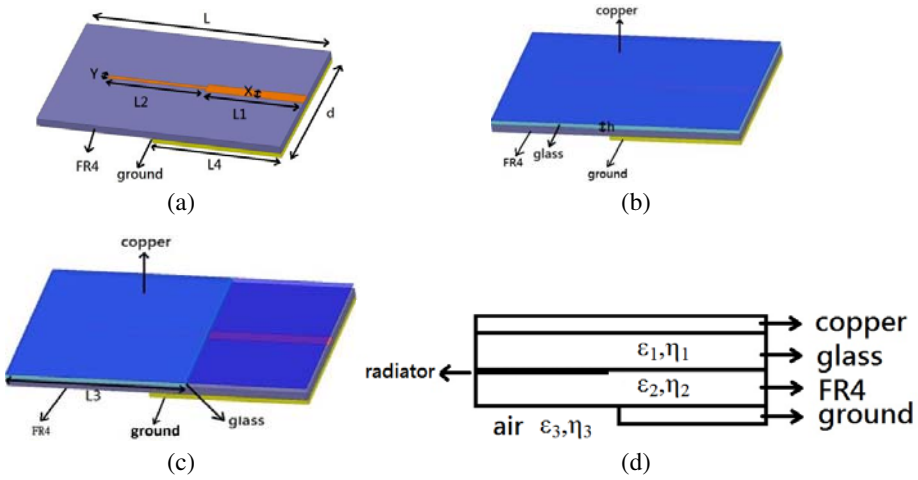

Figure 1. Configuration of monopole antennas: (a) conventional, (b) fully covered with a glass and reflected metal slab, (c) half-covered with a glass and reflected metal slab, (d) the geometry of the profile of the antenna.

2. ANTENNA STRUCTURE AND DESIGN

Figure 1(a) shows the configuration of a conventional monopole antenna (CMA). A fully covered antenna with a glass slab and reflected metal slab is shown in Figure 1(b), and Figure 1(c) shows a half-covered antenna (The half-covered antenna has actually the monopole part covered and the feeding line uncovered). The purpose of analyzing the half-covered antenna is to reduce using glass and copper materials if the enhanced gain of the half-covered antenna is better than the full-covered antenna. Antennas were implemented on an FR4 substrate exhibiting a permittivity of $\varepsilon_r = 4.4$, loss tangent of $\tan\delta = 0.0245$, and thickness of $h = 1.6$ mm. The antenna consists of a monopole, thin glass slab, and reflected metal slab. Figure 1(d) shows the geometry of the antenna profile. The monopole length and strip width are denoted as L_2 and Y, respectively; the dimensions L_2 and Y used are for a quarter-wavelength monopole at the resonant frequency of 2.45 GHz. The length and width of the substrate are denoted as L and d, respectively, and the length and width of the feed line are denoted as L_1 and X, respectively. The length and width of the FR4 substrate are initially selected using the rule of thumb for traditional printed monopole designs. In particular, the width d is used to ensure that the electrical width of the ground plane is greater than half a wavelength at the resonant frequency, and the length L of the substrate is used to ensure that the fringing fields around the truncated end of the monopole do not affect the characteristics substantially. The dimensions were optimized using the high-frequency structure simulator (HFSS) software [12]. An antenna with $d = 32$ mm, $L = 52$ mm, $Y = 0.8$ mm, $L_1 = 21$ mm, $L_2 = 21$ mm, $L_3 = 31$ mm, $L_4 = 27.5$ mm, and $X = 2.4$ mm was used. The geometrical parameters of the antenna are listed in Table 1. A prototype monopole antenna was designed to cover the 2.4-GHz frequency band typically used in wireless local area network (WLAN) applications. The cover was constructed using a 1-mm-thick glass substrate ($\varepsilon_r = 5.2$) that was placed on the monopole antenna.

Table 1. Geometrical parameters of the designed antenna (unit: mm).

L_1	L_2	L_3	L_4	X	Y	L	D
21	21	31	27.5	2.4	0.8	52	32

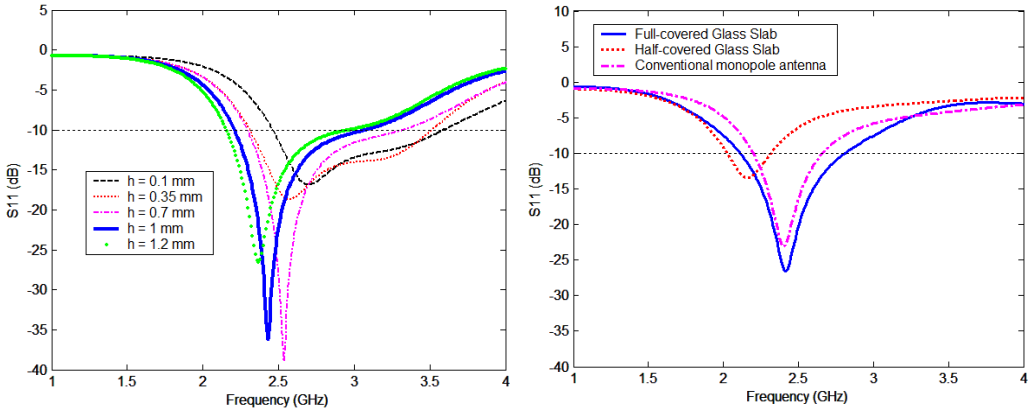

Figure 2. (a) Simulated $|S_{11}|$ (dB) of the optimizing glass slab of thickness h. (b) Simulated $|S_{11}|$ (dB) of the monopole antenna. $h = 1$ mm.

The procedure used to design the gain enhanced antenna, including the monopole antennas, which were fully covered and half-covered with glass slabs, is described below. In addition, the loss tangent of the glass is 0.0038. The configuration of the results in Figures 2–3 employs full-covered and half-covered glass slabs without metal slabs. For the results shown in Figure 2(a), h was used as the adjustment parameter. The glass slab thickness (h) was varied from 0.1 mm to 1.2 mm. The simulated S_{11} (dB) demonstrated that when $h = 1$ mm, the centre frequency was approximately 2.4 GHz, and the return loss was 36.4 dB. The centre frequency of the antenna moved towards a high-frequency band when $h = 0.1$ mm, $h = 0.35$ mm and $h = 0.7$ mm. By contrast, the central frequency of the antenna moved towards a low-frequency band when $h = 1.2$ mm. The downward shift in the resonant frequency with increasing thickness of the glass slab is consistent with the results for larger effective dimensions. Figure 2(b) shows the simulated $|S_{11}|$ (dB) of the antenna fully covered and half covered with glass slabs. For convenient comparison, the simulated $|S_{11}|$ (dB) of the CMA was also included in Figure 2(b). The -10-dB bandwidth of the half-covered antenna was 0.3 GHz (2.02–2.32 GHz). When the antennas fully covered with glass slabs were included, the -10-dB bandwidth was 0.68 GHz (2.12–2.8 GHz). The simulated return loss for the fully covered antenna was between 25 dB and 30 dB. However, the simulated return loss for the half-covered antenna was between 10 dB and 15 dB, and the central frequency moved towards a low-frequency band; therefore, the configuration of the results in Figures 4–10 employs full-covered antenna. Figure 3 shows the 3D gain patterns (not considering the reflected metal slab) of three configuration antennas. The maxima of the 3D gain patterns were 2.43 dB, 2.38 dB, and 2.87 dB for the conventional monopole, half-covered antenna, and fully covered antenna, respectively. As shown in Figure 3, the antenna fully covered with the glass slab exhibited a gain enhancement of approximately 0.64 dB.

The reflected metal slab was constructed using a 0.4-mm-thick copper plate that was placed on the glass substrate. A single glass slab was used, and the dielectric constant of the glass slab was varied to change its reflection magnitude. The gain variation trend fluctuated. When an electromagnetic (EM) wave encounters an interface between two substrates, some of the EM energy is transmitted and some reflected [13]. The reflected EM waves combine with the incident wave, creating constructive or destructive interferences depending on the characteristics of the substrates. Each reflected EM wave corresponds to an image source. These multiple reflections produce multiple images that correspond

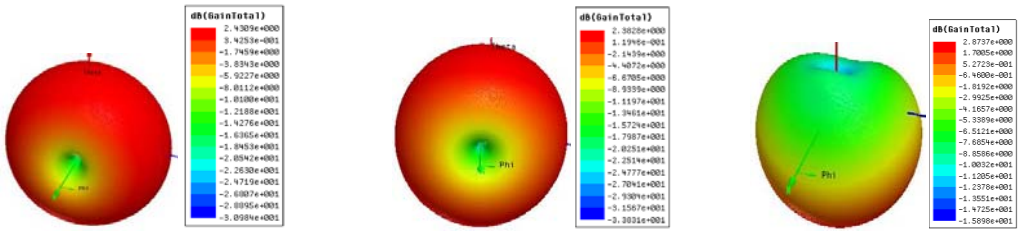

(a) (b) (c)

Figure 3. 3D gain pattern of monopole antennas: (a) conventional monopole antenna, (b) half-covered glass slab monopole antenna, (c) fully covered glass monopole antenna.

to an infinite array. The distance between the substrate and reflected metal slab must enable the EM waves to be projected through the substrate into space and have equal phases in the desired direction of the maximal radiation of the EM waves, which is generally normal to the reflected metal slab. When this basic concept is employed in the design of microstrip antennas, the characteristics of the antenna can be modified to reflect the EM waves. The reflected field can enhance the maximal antenna gain by reducing the EM wave propagation in the substrates. As shown in Figure 1(d), the structure consists of a ground plane, FR4 substrate, glass slab, and reflected metal slab. A horizontal monopole radiator was placed between the glass slab and FR4 substrate at a distance from the reflected metal slab. The intrinsic impedance of a medium can be expressed as [13]

$$\eta = \sqrt{\frac{\mu}{\varepsilon}} \tag{1}$$

where μ is the permeability and ε the permittivity. When an EM wave travels from one medium (glass slab) to a second medium (FR4 substrate) with a different intrinsic impedance, part of the incident power is transmitted into the second medium. Using the intrinsic impedances, the transmission coefficient in the second medium is expressed as [13]

$$t_2 = \frac{2\eta_2}{\eta_1 + \eta_2}, \tag{2}$$

where η_1 and η_2 are the intrinsic impedances for the glass slab and FR4 substrate, respectively. Based on Eqs. (1) and (2), when the dielectric constant (glass slab ε_r) of the glass substrate increases from 4.5 to 8.5 and that of the dielectric constant of the FR4 substrate remains constant at 4.4, the intrinsic impedance decreases, and the transmission coefficient increases; therefore, more power is transmitted into the second medium. When an EM wave travels from the FR4 substrate (η_2) to the air (η_3), the transmission coefficient in the air is

$$t_3 = \frac{2\eta_3}{\eta_2 + \eta_3}, \tag{3}$$

where η_3 is the intrinsic impedance for the air. The more power is transmitted into the second medium (FR4 substrate), the more power is transmitted into the third medium (air) when η_2 and η_3 are fixed. As shown in Figure 4(a), the gain fluctuates with the dielectric constant ε_r of the glass, and peaks initially at a dielectric constant $\varepsilon_r = 5.2$. The dielectric constant ε_r varies from 4.5 to 8.5. In the current study, the gain peaked near the dielectric constant $\varepsilon_r = 7.75$. However, the gain decreased rapidly when the dielectric constant was higher than 8.1 because of multiple reflection effects [13]. This result is shown clearly in Figure 4(a). In addition, in the same studies, the thickness of the glass slab has been varied to change its reflection magnitude. The results shown in Figure 4(b) indicate that the antenna gain increases as the thickness of the glass slab increases until it is thicker than 1 mm. The simulated results of gain versus the thickness of the glass slab showed that a gain level of > 4 dBi was achieved as long as the thickness of the glass slab was 1 mm. The gain was slightly larger than that shown in Figure 4(a) when the glass slab thickness was 1 mm. As shown in Figures 4(a) and 4(b), the gain clearly oscillates with the dielectric thickness h and dielectric constants. The simulated 3D gain patterns of both the CMA and dielectric constant $\varepsilon_r = 7.75$ gain enhancement antenna based on the HFSS software are illustrated in Figure 5. Clearly, the dielectric constant $\varepsilon_r = 7.75$ gain enhancement antenna yields a

more directional pattern than that for the CMA. The maximal 3D gain was approximately 5.1 dBi. The 3D gain patterns indicated an enhancement of approximately 2.67 dB when the glass slab and reflected metal slab were used. In summary, when thickness of the glass slab is 1 mm and dielectric constant 7.75, an acceptable antenna gain can be expected. In addition, the dielectric constant ε_r of the glass was measured using the Speag dielectric assessment kit (DAK) series, which enables the probe to be moved within the media under the test to measure the dielectric constant directly and the thickness of the glass slab precisely by employing a feeler gauge.

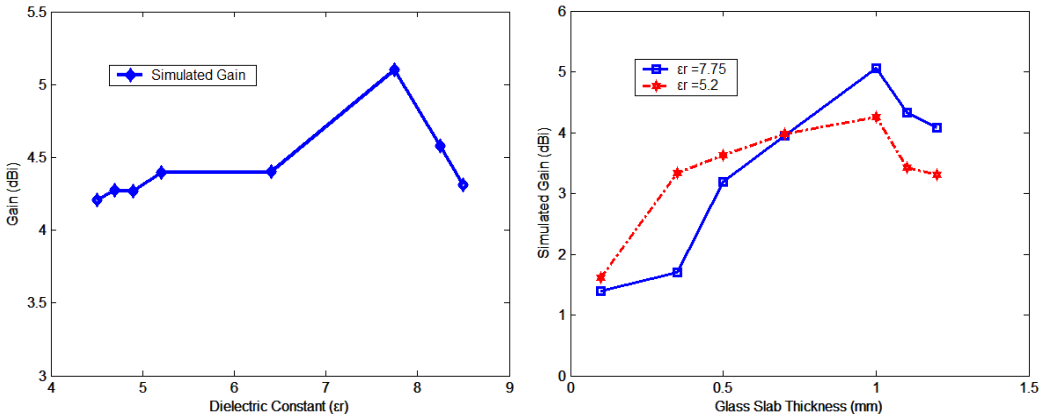

(a) (b)

Figure 4. (a) Gain versus dielectric constant of the antenna with a glass slab. $h = 1$ mm. (b) Gain versus glass slab thickness of this antenna.

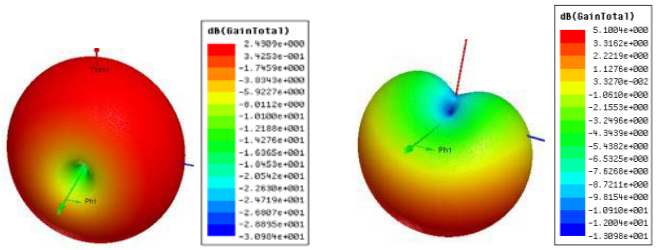

(a) (b)

Figure 5. 3D gain pattern of antennas: (a) CMA, (b) gain enhancement antenna with dielectric constant $\varepsilon_r = 7.75$.

3. EXPERIMENTAL RESULTS

Figures 6(a), 6(b), and 6(c) show photographs of the top, bottom, and side views of the fabricated antenna, respectively. The antenna volume was $3 \times 32 \times 52\,\text{mm}^3$. The return loss was measured using an Agilent N5230A network analyzer. Figure 7 shows the measured $|S_{11}|$ (dB) of the antenna with a glass slab of dielectric constant $\varepsilon_r = 7.75$, dielectric constant $\varepsilon_r = 5.2$, and that of the CMA.

For effective comparison, the geometrical parameters of the antennas were adjusted to enable the antennas to attain their approximate resonant frequencies. The measured $|S_{11}|$ (dB) indicated that the -10-dB bandwidth for the 2.4-GHz frequency band range of the antenna with a glass slab of dielectric constant $\varepsilon_r = 7.75$ was 2.27–2.61 GHz (0.34 GHz). The measured -10-dB bandwidth of the antenna with a glass slab of dielectric constant $\varepsilon_r = 5.52$ was 0.28 GHz (2.27–2.55 GHz). The measured $|S_{11}|$ (dB) sink of the proposed antenna was < -25 dB at the 2.4-GHz WLAN bands (2.4–2.4835 GHz). The measured results of the proposed antenna concurred with those of the CMA.

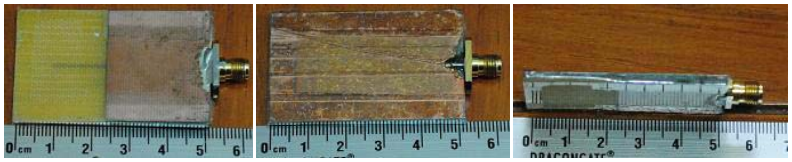

(a) (b) (c)

Figure 6. Fabricated gain enhanced planar monopole antenna. (a) Top view. (b) Bottom view. (c) Side view.

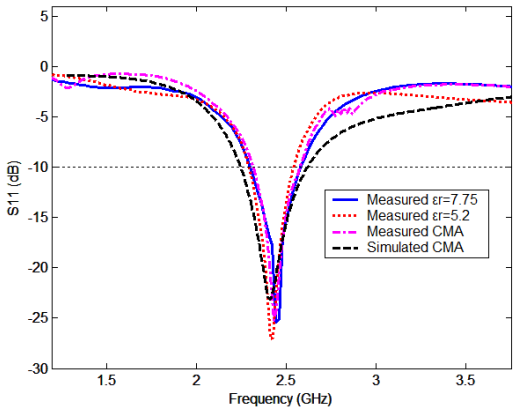

Figure 7. Measured $|S_{11}|$ (dB) of the antennas with dielectric constants $\varepsilon_r = 7.75$ and 5.2, and measured and simulated $|S_{11}|$ (dB) of the CMA.

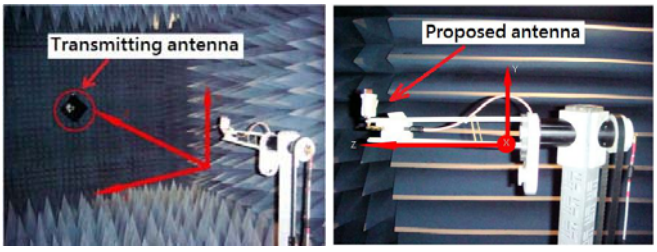

(a) (b)

Figure 8. Photographs of the experimental environment for gain, radiation efficiency, and field pattern measurements. (a) Transmitting antenna (b) Proposed antenna.

Photographs of the experimental environment for gain, radiation efficiency, and field patterns measurement are shown in Figure 8. Figure 9(a) shows the measured gain of the CMA and the proposed antenna with dielectric constants $\varepsilon_r = 7.75$ and 5.2. The frequencies ranged from 2.4 GHz to 2.63 GHz. The peak gain for the 2.4-GHz frequency band was obtained. The highest gain was approximately 5 dBi at 2.45 GHz for dielectric constant $\varepsilon_r = 7.75$ antenna, 2.5 dBi for the measured CMA, 2.6 dBi for the simulated CMA, and 4.3 dBi for the dielectric constant $\varepsilon_r = 5.2$ antenna. The slight difference between the measured and simulated gains of the CMA for higher frequencies as seen in Figure 9(a) was due to conductor and dielectric losses of the circuit substrate, limitations in manufacturing technology, as well as parasitic effects from soldering.

The gain could be increased to 2.5 dBi when the glass and reflected metal slabs were used. Figure 9(b) shows the measured radiation efficiency for antenna with dielectric constants $\varepsilon_r = 7.75$ and 5.2. The highest efficiency was 71.617% at 2.45 GHz for the dielectric constant $\varepsilon_r = 7.75$ antenna, and 56% at 2.45 GHz for the dielectric constant $\varepsilon_r = 5.2$ antenna. The 2D E-plane patterns (CoPol.) showed a gain enhancement of approximately 2.5 dB at 2.45 GHz. Compared with the CMA (Figure 1),

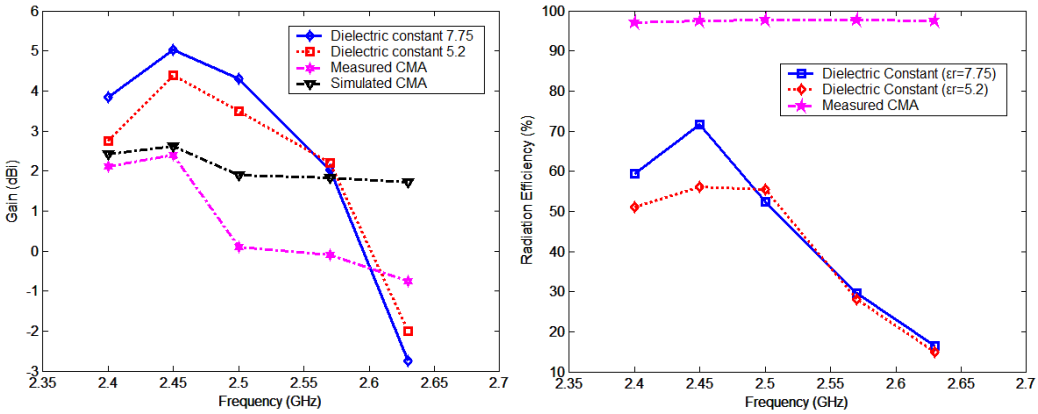

Figure 9. (a) Measured gains of antenna with dielectric constants $\varepsilon_r = 7.75$ and 5.2, and measured and simulated gains of the CMA (b) Measured radiation efficiency for antennas with dielectric constant $\varepsilon_r = 7.75$, $\varepsilon_r = 5.2$, and the CMA.

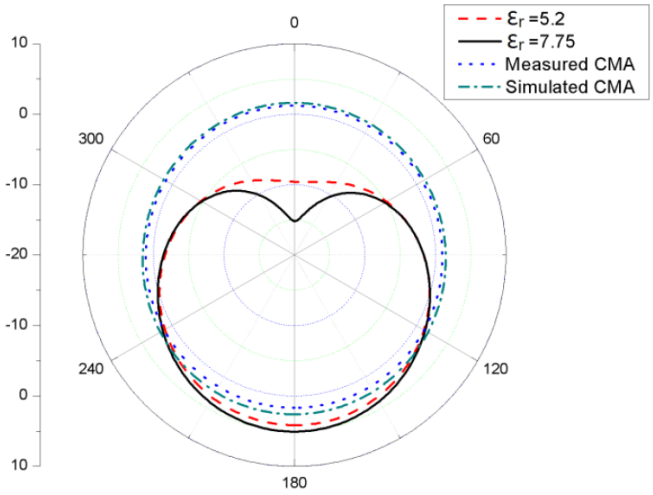

Figure 10. 2D E-plane patterns of the antenna with dielectric constants $\varepsilon_r = 5.2$, $\varepsilon_r = 7.75$, the measured CMA, and the simulated CMA at 2.45 GHz.

adding the glass and reflected metal slabs enables the proposed antenna to concentrate more radiation power in one direction and reduce the radiation power towards the two sides and the back of the proposed antenna. The advantages of using a glass slab instead of a commercial microwave laminate are low cost (approximately \$1) and obtaining the dielectric constants not to be limited by the laminates of manufacturers. The additional space required, gain enhancement, structure, and cost of the proposed antenna (dielectric constant $\varepsilon_r = 7.75$) are compared with previously reported gain enhancement antennas in Table 2. In Table 2, the additional space required for the proposed antenna is reduced by up to 97.8% of [3, 6–11], 96.3% of [2, 5], 95.6% of [1], and 57.7% of [4]. The gain enhancement of the proposed antenna is more than 0.9 dB of [2] and 0.77 dB of [4]. The proposed antenna has a simpler structure and lower cost than the previously reported antennas.

The novel configuration relates to the mechanism of disposing the proposed antenna for disposing a glass and reflected metal slab on a wireless communication device. The proposed antenna can comprise a kinematic chain attachable to the wireless communication device corresponding to the antenna. Normally, the radiation pattern of the monopole antenna is nearly omnidirectional in the operating frequency band; therefore, when communication devices are located in a poor coverage area, the antenna

Table 2. Additional space, gain enhancement, structure, and cost of the proposed antenna and those of other reports.

Gain enhancement ant.	additional space	Gain enhancement	cost	Structure
Proposed ant.	$\sim 0.011\lambda_0$	2.5 dB	very low ($\sim$ \$1)	simple
PRS ant. [6–11]	$\sim 0.5\lambda_0$	about 15 dB	very high	complicated
Rivera-Albino et al.	$\sim 0.25\lambda_0$	4 dB	high	complicated
Lai et al. [2]	$\sim 0.3\lambda_0$	1.6 dB	medium	Simple
Chung et al. [3]	$\sim 0.5\lambda_0$	3 dB	high	complicated
Yang et al. [4]	$\sim 0.026\lambda_0$	1.73 dB	very high	complicated
Moharamzade et al. [5]	$\sim 0.3\lambda_0$	2.5 dB	high	complicated

can obtain gain enhancement in certain directions depending on the protruding wireless communication device where the glass and reflected metal slabs are disposed.

4. CONCLUSIONS

This paper proposes a novel configuration gain enhancement monopole antenna with a radiation pattern that achieves gain enhancement by employing a thin glass slab and reflected metal slab on the monopole antenna structure. Based on the optimization by using the HFSS software, gain was enhanced using suitable combinations of glass slab thickness and dielectric constants. The monopole antenna gain increased to approximately 5 dBi without compromising the bandwidth. The results obtained for the directional pattern, return loss, gain, and radiation efficiency of the proposed antenna were analyzed. The measured results are consistent with the simulated ones.

ACKNOWLEDGMENT

This work was supported by the National Science Council, R.O.C., under Grant NSC 102-2221-E-262 -002.

REFERENCES

1. Rivera-Albino, A. and C. A. Balanis, "Gain enhancement in microstrip patch antennas using hybrid substrates," *IEEE Antenna Propagat. Lett.*, Vol. 12, 476–479, 2013.
2. Lai, W.-C., A.-C. Sun, N.-W. Chen, and C.-W. Hsue, "Gain enhancement of planar monopole with magnetodielectric material," *Progress In Electromagnetics Research C*, Vol. 21, 179–190, May 2011.
3. Chung, K. L. and S. Kharkovsky, "Mutual coupling reduction and gain enhancement using angular offset elements in circularly polarized patch array," *IEEE Antenna Wireless Propagat. Lett.*, Vol. 12, 1122–1124, 2013.
4. Yang, W., W. Che, and H. Wang, "High-gain design of a patch antenna using stub-loaded artificial magnetic conductor," *IEEE Antenna Wireless Propagat. Lett.*, Vol. 12, 1172–1175, 2013.
5. Moharamzadeh, E. and A. M. Javan, "Triple-band frequency-selective surfaces to enhance gain of X-band triangle slot antenna," *IEEE Antenna Wireless Propagat. Lett.*, Vol. 12, 1145–1148, 2013.
6. Ge, Y., K. P. Esselle, and T. S. Bird, "The use of simple thin partially reflective surfaces with positive reflection phase gradients to design wideband, low-profile EBG resonator antennas," *IEEE Trans. Antennas Propagat.*, Vol. 60, No. 2, 743–750, Feb. 2012.
7. Weily, A. R., T. S. Bird, and Y. J. Guo, "A reconfigurable high-gain partially reflecting surface antenna," *IEEE Trans. Antennas Propagat.*, Vol. 56, No. 11, 3382–3390, Nov. 2008.

8. Debogović, T., J. Bartolić, and J. Perruisseau-Carrier, "Dual-polarized partially reflective surface antenna With MEMS-based beamwidth reconfiguration," *IEEE Trans. Antennas Propagat.*, Vol. 62, No. 1, 228–236, Jan. 2014.
9. Debogović, T. and J. Perruisseau-Carrier, "Array-fed partially reflective surface antenna with independent scanning and beamwidth dynamic control," *IEEE Trans. Antennas Propagat.*, Vol. 62, No. 1, 446–449, Jan. 2014.
10. Hosseini, A., F. Capolino, F. De Flaviis, P. B. G. Lovat, and D. R. Jackson, "Improved bandwidth formulas for Fabry-Pérot cavity antennas formed by using a thin partially-reflective surface," *IEEE Trans. Antennas Propagat.*, Vol. 62, No. 5, 2361–2367, May 2014.
11. Vaidya, A. R., R. K. Gupta, S. K. Mishra, and J. Mukherjee, "Right-hand/left-hand circularly polarized high-gain antennas using partially reflective surfaces," *IEEE Antenna Wireless Propagat. Lett.*, Vol. 13, 431–434, 2014.
12. HFSS 13, Ansoft Corporation (ANSYS), Available: www.ansoft.com.
13. Cheng, D. K., *Fundamentals of Engineering Electromagnetics*, 2nd edition, Addison Wesley, 1993.